◆ Human Brain Mapping 8:194–208(1999) ◆

Measuring Phase Synchrony in Brain Signals

Jean-Philippe Lachaux, Eugenio Rodriguez, Jacques Martinerie, and Francisco J. Varela*

Laboratoire de Neurosciences Cognitives et Imagerie Cérébrale, CNRS UPR 640
Hôpital de La Salpêtrière, Paris, France

Abstract: This article presents, for the first time, a practical method for the direct quantification of frequency-specific synchronization (i.e., transient phase-locking) between two neuroelectric signals. The motivation for its development is to be able to examine the role of neural synchronies as a putative mechanism for long-range neural integration during cognitive tasks. The method, called phase-locking statistics (PLS), measures the significance of the phase covariance between two signals with a reasonable time-resolution (<100 ms). Unlike the more traditional method of spectral coherence, PLS separates the phase and amplitude components and can be directly interpreted in the framework of neural integration. To validate synchrony values against background fluctuations, PLS uses surrogate data and thus makes no a priori assumptions on the nature of the experimental data. We also apply PLS to investigate intracortical recordings from an epileptic patient performing a visual discrimination task. We find large-scale synchronies in the gamma band (45 Hz), e.g., between hippocampus and frontal gyrus, and local synchronies, within a limbic region, a few cm apart. We argue that whereas long-scale effects do reflect cognitive processing, short-scale synchronies are likely to be due to volume conduction. We discuss ways to separate such conduction effects from true signal synchrony. *Hum Brain Mapping 8:194–208, 1999.*

Key words: neural synchrony; phase-locking; coherence; EEG; EcoG; epilepsy; gamma-band; deblurring

INTRODUCTION

Cognitive acts require the integration of numerous functional areas widely distributed over the brain and in constant interaction with each other [Friston et al., 1997; Tonini and Edelman, 1998]. It has become a topic of much interest to explore the possibility that such large-scale integration could be mediated by neuronal groups that oscillate in the gamma range (30–80 Hz, also referred to as 40 Hz) that enter into precise phase-locking over a limited period of time. (Hereafter, we refer to these phenomena simply as "synchrony" or "phase synchrony".) Whence the importance for a reliable and robust method for directly measuring such phase synchrony in this frequency band for experimentally recorded biological signals, which are not spikes, but local field potentials (LFP) of various degrees of spatial resolution. The purpose of this report is to introduce, for the first time, an effective method to estimate the instantaneous phase relationship between two neuroelectric or biomagnetic signals and to apply it to intracortically recorded signals in humans. We also introduce the required statistical means to test the validity of the measured synchrony against the background fluctuations in a given experimental situation.

The role of synchronization of neuronal discharges, although not a new idea, has been greatly highlighted by results from microelectrodes in animals [see, e.g.,

Contract grant sponsor: DRET; Contract grant sponsor: Human Science Frontier.

*Correspondence to: Dr. Francisco J. Varela, LENA-CNRS UPR 640, Hôpital de La Salpêtrière, 47 Bd de l'Hôpital, 75651 Paris cedex 13, France. E-mail: fv@ccr.jussieu.fr

Received for publication 13 March 1998; accepted 17 May 1999

Singer and Gray, 1995]. In fact, two scales of phase synchrony can be distinguished: most animal studies based on microelectrode recordings have dealt with *short-range* synchronies [e.g., Gray et al., 1989; Neuenschwander et al., 1996], or between adjacent areas corresponding to a single sensory modality [e.g., König et al., 1995]. These local synchronies have been interpreted most commonly as subserving "perceptual binding.'' More recently, evidence has also been found for *long-range* synchronizations between widely separated brain regions [Roelfsema et al., 1997]. This is in agreement with the more general notion that phase synchrony should subserve not just binding of sensory attributes, but the overall integration of all dimensions of a cognitive act, including associative memory, emotional tone, and motor planning [Damasio, 1990; Varela, 1995].

These multiunit studies in animals have been complemented by studies at coarser levels of resolution in humans and animals. In fact, gamma band responses can be recorded during visual discrimination protocols on the human scalp [Tallon-Baudry et al., 1997] and in subdural electrocorticograms [Le van Quyen et al., 1997; Lachaux et al., 1999a]. One can distinguish an early (100 ms) response phase-locked to the stimulus or *evoked* response, and a later (200 ms) *induced* response nonphase-locked to the stimulus. Both these responses necessarily imply a degree of local phase-locking, since otherwise no signal would reach the surface of cortex or scalp with enough amplitude. They would annihilate due to the summation of phases distributed very broadly. Thus there is some evidence to suggest that synchronization mechanisms as those found in single-unit studies in animals also occur at large scales recorded with macroelectrodes; they are long-range synchronies.

However, the quantification of phase synchrony between macroelectrodes (EEG / MEG or intracortical recordings) requires methods that are entirely different that the cross-correlograms between spike discharges that suffice for microelectrode studies. This is the main purpose of the present study. But in this context, it is important to distinguish very sharply between synchrony (as defined above) and the classical measures of spectral covariance or *coherence* that have been extensively used elsewhere [Bullock and McClune, 1989; Bressler et al., 1993; Menon et al., 1996]. Unfortunately, coherence is a measure that does not separate the effects of amplitude and phase in the interrelations between to signals. This point is discussed in detail later, but the novelty of our results is to a large extent simply to arrive at a measure where the phase component is obtained *separately* from the amplitude component for a given frequency. Only then can one proceed to test the synchrony hypothesis for brain integration. In a separate work, we have successfully applied the present method for the detection of gamma synchronies over the scalp during visual perception [Rodriguez et al., 1999]. Here, we present the methods in extenso on the basis of simulations and intracortical recordings as an ideal test case.

This report is divided into three main sections. The first introduces a new technique for phase-locking detection: the phase-locking statistics (PLS). The second section applies PLS to LFP data from human intracortical recordings. In the third section, we examine the problem of volume conduction and the choice of a reference electrode, the two main difficulties associated with the interpretation of synchrony results.

QUANTIFICATION OF PHASE-LOCKING

Phase-locking statistics

Here, we introduce our method of detecting synchrony in a precise frequency range between two recording sites. This method uses responses to a repeated stimulus and looks for latencies at which the phase difference between the signals varies little across trials (phase-locking). Given two series of signals x and y and a frequency of interest f, the procedure computes for each latency a measure of phase-locking between the components of *x* and *y* at frequency f (we call this measure phase-locking value, or PLV). This needs the extraction of the instantaneous phase of every signal at the target frequency. The procedure follows three steps (Fig. 1).

Step 1. We band-pass filter (finite impulse response of length = 300 ms) each signal between (f ± 2 Hz).

Step 2. We compute its convolution with a complex Gabor wavelet centered at frequency f:

$$G(t, f) = \exp\left(-\frac{t^2}{2\sigma_t^2}\right) \exp\{j2\pi ft\}.$$

Following Grossman [1989], we chose $\sigma_t = 7/f$. For instance, σ_t = 140 ms for f = 50 Hz. The phase of this convolution $\phi(t, n)$ is extracted for all time-bins t, trial n [1, . . . , N], and for each of the pair of electrodes.

The phase locking value (PLV) is then defined at time t as the average value:

$$PLV_t = \frac{1}{N}\left|\sum_{n=1}^{N} \exp\left(j\theta(t, n)\right)\right|$$

where $\theta(t, n)$ is the phase difference $\phi_1(t, n) - \phi_2(t, n)$. PLV measures the intertrial variability of this phase

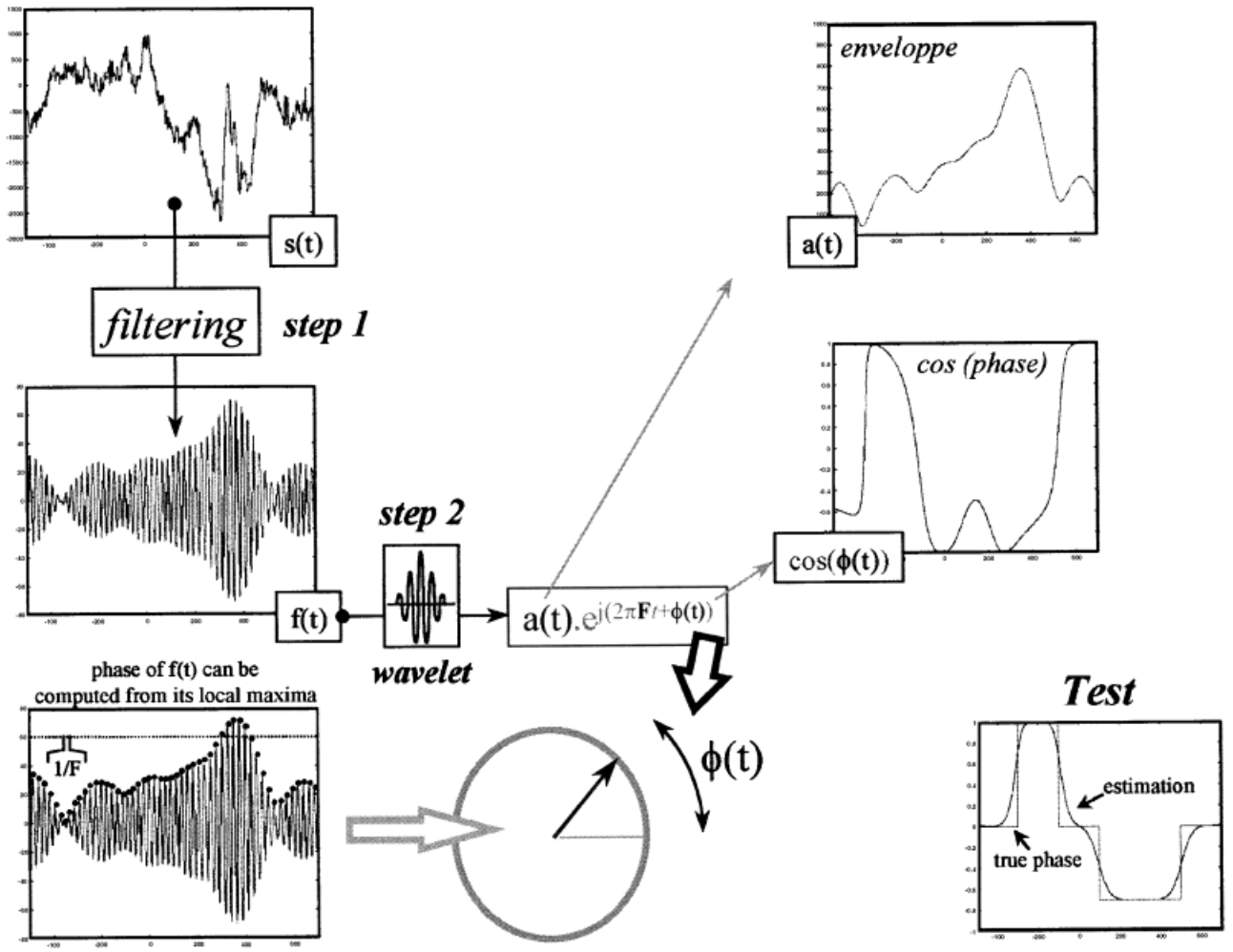

Figure 1.

Evaluation of the instantaneous phase of a signal for a frequency f. As a first step, the raw signal s (t) is band-pass filtered to generate f(t) (step 1); the convolution of f(t) with a Morlet wavelet centered at frequency F provides the envelope a(t) and the instantaneous phase $\phi(t)$ (step 2). $\phi(t)$ can also be inferred (bottom left) from a comparison between the latencies of f's maxima (black points) and reference time markers (black ticks separated by a constant interval: 1/f). Both methods give the same results. To test the methods, we generated a signal $x(t) = \sin(2\pi Ft + \theta(t))$, with abrupt phase variations, and computed $\phi(t)$, an estimator of $\theta(t)$. On the bottom right, inset shows $\cos(\theta(t))$ (rectangular function) together with $\cos(\phi(t))$ (smooth approximation).

difference at t: If the phase difference varies little across the trials, PLV is close to 1; it is close to zero otherwise (Fig. 2). This procedure can be repeated for several frequencies in order to study a broader frequency range.

Step 3. The third step, or ''test,'' is to build a statistical test based on surrogate data [Theiler et al., 1992, Müller-Gerking et al., 1996] to differentiate significant PLV against background fluctuations. Formerly, we test our samples of phase differences for randomness against a unimodal distribution with an unspecified mean direction. The Raleigh test can be used [Fisher, 1993] to test the H_0 hypothesis that our samples are drawn from a uniform distribution. However, in our case, the sampling distribution of a statistic is not known and we cannot assume uniformity. This can be seen in a simple example. Let us assume two independent neural populations that start to oscillate at 40 Hz in response to stimulation after a random delay of 50–55 ms. The phase of these oscillations at 55 ms will vary from trial to trial from 0–90° (5 ms is about a quarter of a cycle at 40 Hz). Therefore, the phase difference between these two neural groups will reach values only between −90° and 90°, which is not uniform. Yet, a Raleigh test would conclude that the phase differences are not uniformly distributed and

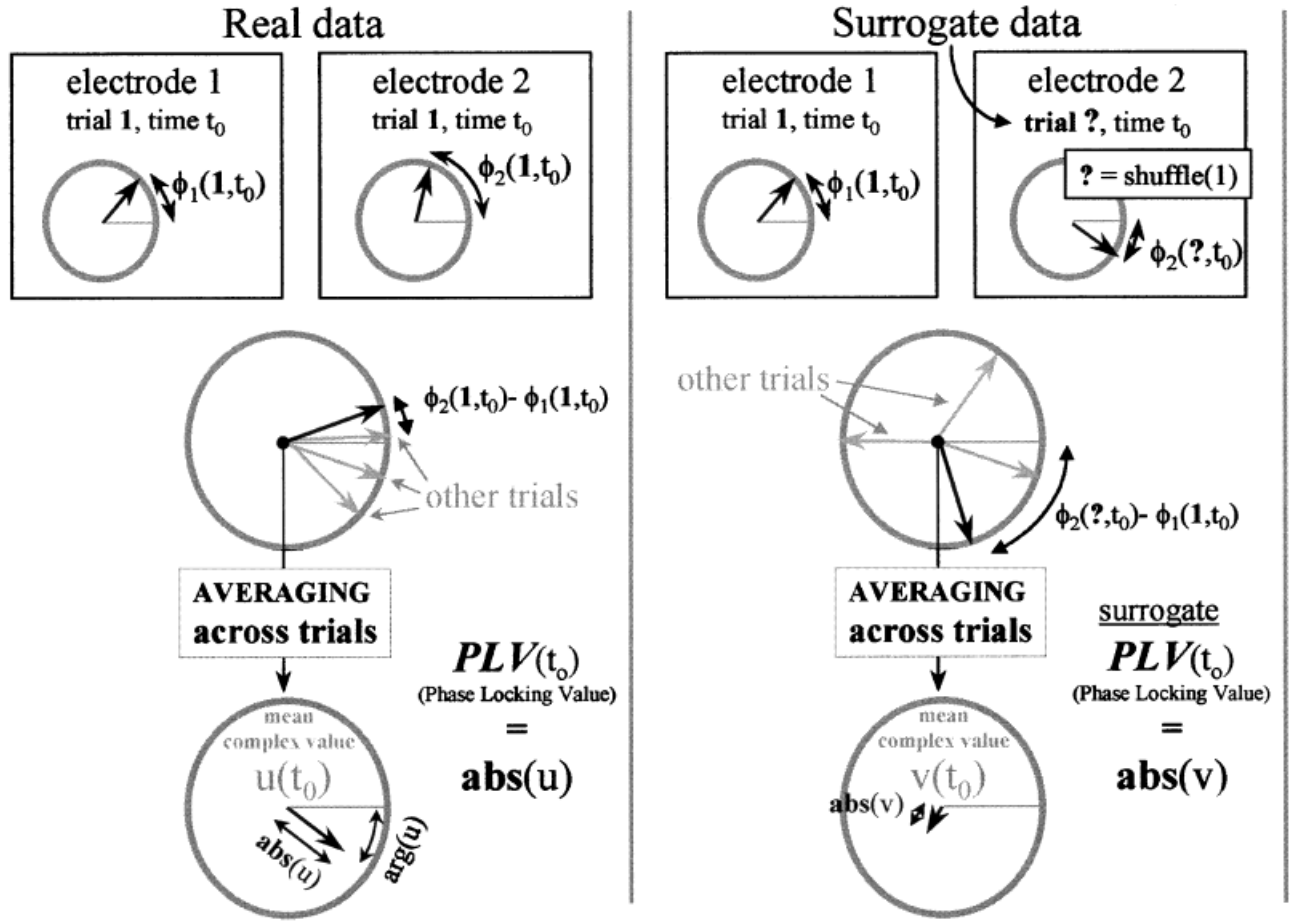

Figure 2.

Estimation of phase-locking value. Left: Our synchrony index is directly related to the intertrial variability of the phase differences between two electrodes (see description of the method for details). By averaging these phase differences across the trials, we obtain a complex value u (for each latency t), which amplitude (abs (u)) is the phase-locking value. Right: Surrogate data are constructed by shuffling the trials of one of the electrodes (see text for details).

would detect a phase-locking between the groups. When the sampling distribution of a statistic is unknown, one must rely on recent techniques of randomization, or bootstrap [Fisher, 1993]. Our statistical test is based on randomization and is adapted to our particular set of data.

The main advantage of this approach is that it does not require any a priori hypothesis on the signals. We test the H_0 hypothesis that the two series of phase values $\phi_1(n)$ and $\phi_2(n)$ are independent. For this purpose, we generate 200 new series of variables, which have the same characteristics as the original signal coming from electrode 2, except that we built them to be independent of the signals coming from electrode 1. These series are created by shuffling the trials within the measures of electrode 2 to make new series $y'(n) = y(\text{shuffle}(n))$, where (y(i) is the signal recorded at electrode 2 during trial i (Fig. 2).

For each surrogate series y′, we measure the maximum between x and y′ in time. These 200 values are used to estimate the significance of PLV between the original signals x and y. The proportion of surrogate values higher than the original PLV (between x and y) for a time t is called phase-locking statistics (PLS). It measures the probability of having false positives for a given level of significance. In this study, we used a criterion of 5% (PLS $<$ 5%) to characterize significant synchrony, but this is, of course, a function of the required rigor of significance in the context of the signals being studied. Our method is related to an approach proposed by Friston et al. [1997] to quantify MEG data. In fact, they propose to estimate the

correlation coefficient between two signals at a precise frequency, which implies a degree of phase-locking. Also, their statistical analysis was markedly different from ours.

Some comments are in order. In step 1, one may wonder if the filtering step is not redundant with the wavelet convolution and if it does not introduce artifacts. It seems that $\phi(t, n)$ could be obtained directly by a convolution of the wavelet with the *unfiltered* signal (call this method A), instead of using a filtering step prior to the convolution (method B). In fact, both methods were tested and led to slightly different results. We could make the following verifications of method B: (1) when transient 40 Hz oscillations easily could be seen in raw (unfiltered) data, we checked that the latencies of their peaks were identical with those of the filtered signals, and (2) when the filtered signal had clear oscillations, its exact phase could be read straightforwardly from the latencies of the maxima of these oscillations (this direct lag estimation is slow, but highly reliable). By comparing this phase with our evaluation, we could check the exactness of method B. Since method A occasionally gave different results, we relied on method B.

In step 3, the statistical method we use should detect any significant phase synchrony between two electrodes, except in one important case: when the phase values $\phi_1(n)$ *and* $\phi_2(n)$ remains constant across the trials. In that situation, shuffling the trials within the measures of electrode 2 does not change the phase-locking value, whereas signals are actually synchronous. These false negatives easily can be detected since they are associated with high PLV. Also, they easily can be detected using simpler techniques that estimate the intertrial variability of the phase of each electrode as recently proposed [Tallon-Baudry et al., 1996; Lachaux et al., 1999a].

Why not use coherence?

Most studies that have attempted directly to study the putative importance of synchrony so far have employed a measure traditionally called frequency coherence (or more specifically, magnitude squared coherence, MSC) [Clifford Carter, 1987]. Thus the improvements provided by PLS are best seen in contrast to MSC. The most salient differences are twofold.

Coherence can be applied only to stationary signals. Coherence is a measure of the linear co-variance between two spectra. In particular, for each frequency f, the MSC is defined for two zero-mean stochastic processes by the squared modulus of their cross-spectral density at frequency f, normalized by their respective auto-spectra. These spectra can be *estimated* from *finite* sets of data by: (1) subdividing the whole data sets into segments, (2) computing approximations of the spectra of each segment using a DFT (Discrete Fourier Transform), and (3) averaging these subspectra across all the segments. The quality of the estimation depends on the number and size of the segments [Clifford-Carter, 1987]. Segments are usually successive time intervals, defined by a window sliding in time over the whole recording. In that case, a single measure of coherence typically needs several seconds of data, which limits the temporal resolution of the method. However, for protocols with repeated stimulations, coherence can be computed with a much better resolution because the window that defines the segments can be slided across trials instead of being slided in time (event-related coherence). Yet, both methods require that each segment of data correspond to the same process with the same spectral properties. Since this assumption of *stationarity* (in time or across trials) can rarely be validated, we prefer a measure of phase-locking that does not require stationarity.

Coherence does not specifically quantify phase-relationships. Coherence also increases with amplitude covariance, and the relative importance of amplitude and phase covariance in the coherence value is not clear. Since phase-locking is sufficient to conclude that two brain regions interact, it is important to develop alternative measures for the sole detection of phase covariance. In fact, there is no clear interpretation for the changes in coherence between two neural signals, beyond an obvious indication of interdependency.

In addition, the classic statistical analysis of coherence is not based on a comparison with trial-shifted surrogate data, but rather on a comparison with independent white noise signals [Clifford-Carter, 1987]. Therefore, coherence statistics test the H_0 hypothesis that pairs of neural signals behave like independent *white-noise* signals. Since neural signals are not white-noise signals, this H_0 hypothesis might be too strong and might be rejected too easily.

Simulations

We first tested PLS with two series of signals phase-locked during two well-defined intervals in order to validate its temporal resolution. These signals were derived from two independent series of 50 signals obtained from intracortical recordings of an epileptic patient (see next section) ($s_1(t, n = 1 \ldots 50)$ and $s_2(t, n = 1 \ldots 50)$, totaling 50 responses to two different stimuli measured in two different brain loca-

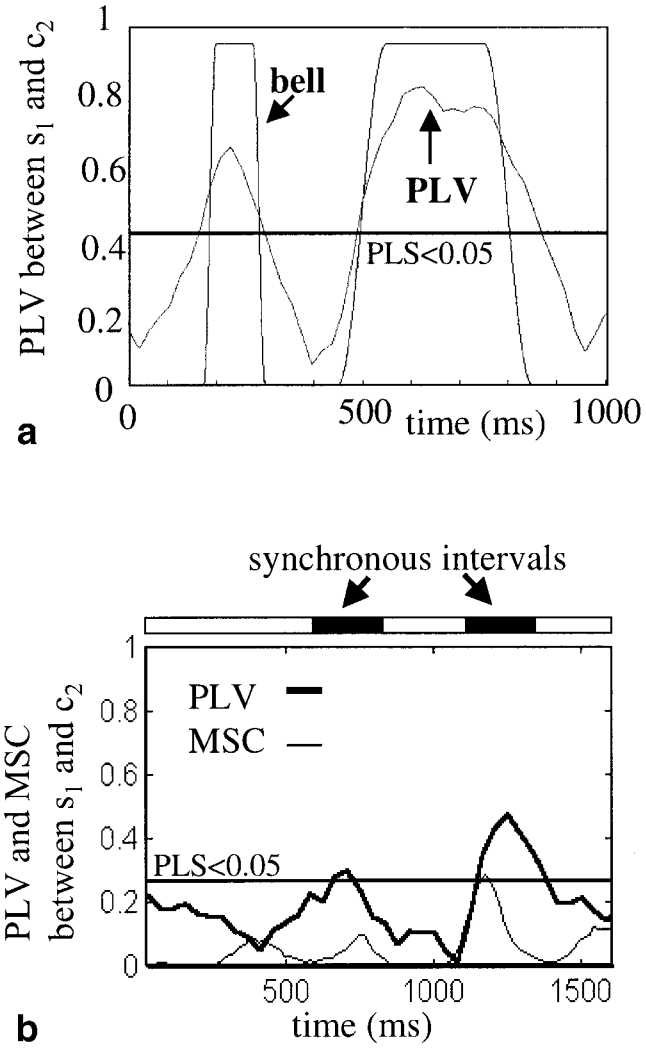

Figure 3.
(**a**). Estimation of PLV's temporal resolution. Two periods of high synchrony are simulated. Synchrony periods are characterized by nonzero values of the bell function (see text for details). Values are plotted as a function of time; values above the horizontal line are significant (PLS $<$ 0.05). Synchrony can be detected in segments as short as 75 ms. (**b**). Estimation of PLV's detection resolution. As in Figure 3, two periods of high synchrony are simulated (nonzero values of the bell function (see text for details). PLV and MSC values are plotted as a function of time; PLV above the horizontal line are significant (PLS $<$ 0.05). During periods of low amplitude co-variance, MSC gives a false negative.

tions. We applied a finite impulse response band-pass filter (41–45 Hz) to s_1 and s_2 to generate two new series s_1^ω and s_2^ω and computed a third series $c_1^\omega = Bell \cdot s_1^\omega + (1 - Bell \cdot) \cdot s_2^\omega$. (*Bell* was a function always equal to zero, except during two periods of 75 ms and 200 ms where it was equal to 1 (Fig. 3.)

Signal s_2 was then modified into $c_2 = s_2 - s_2^\omega + c_1^\omega$, a signal synchronous with s_1 (41–45 Hz) during two short intervals. We computed PLS between s_1 and c_2 (target frequency = 43 Hz) to test whether this method could detect and separate these two episodes. As shown in Figure 3a, the temporal resolution of PLS was precise enough to do so. It can, therefore, be used to detect short episodes of synchrony (in this case, three oscillation cycles at 40 Hz, 75 msec) with a relatively small number of trials (50).

We devised a second simulation intended to illustrate the inability MSC to separate phase and amplitude covariance. We used two series of signals phase-locked during two well-defined intervals, but with independent amplitudes. We expected that a lack of amplitude covariance would induce MSC ignore synchrony, but not PLS.

This simulation was very similar to the previous one: using two independent series (50 trials) of data s'_1 and s'_2, we repeated the above procedure to generate two series s'^ω_1 and s'^ω_2 and a third series $c'^\omega_1 = Bell' \cdot s'^\omega_1 + (1 - Bell' \cdot) \cdot s'^\omega_2$. (In this case, *Bell′* had two nonzero periods lasting 200 ms each.) s_2 was this time modified into $c_2 = s_2 - s_2^\omega + random \cdot c_1^\omega$, where random was a value randomly chosen between 0 and 1 and different for each trial. This number was introduced to make the amplitudes of the signals independent, so that synchronous periods specified by *Bell′* corresponded solely to phase-coupling and not to amplitude covariance. The results of this simulation are shown in Figure 3b; as expected, MSC was reduced to the level of noise during the first episode of synchrony. In contrast, PLS detects both episodes of synchrony correctly.

Interestingly, in our simulations MSC did not give false positives when there was amplitude covariance, but not phase locking. Thus our tentative conclusion so far is that MSC is fooled specially by synchronies that are not accompanied by high amplitude covariances.

MEASURING SYNCHRONIES IN HUMAN INTRACORTICAL RECORDINGS

Subjects and recordings

Here, we examine the results of applying PLS to subdural recordings of an epileptic patient performing a visual discrimination task. Details of the experimental conditions can be found elsewhere [Lachaux et al., 1999a]. This right medial temporal epilepsy patient (subject PI) required intracranial EEG monitoring to confirm the exact site of the epileptogenic zone before surgical treatment. Four electrodes plots, each with eight recording sites, were inserted along occipito-

TABLE I. Electrodes positions for subject PI*

1. R anterior amygdalia	19. R anterior cingulate gyrus
2. R hippocampus—head	20. R frontal superior gyrus
3. R hippocampus—anterior	21. R frontal superior gyrus
4. R hippocampus—body	22. R frontal superior gyrus
5. R white matter	23. R front superior gyrus / arachnoide space
6. R white matter	24. R perimeningeal space
7. R temporo-occipital sulcus	25. L medio orbital gyrus / olfactory sulcus
8. R temporo-occipital gyrus	26. L anterior cingulate gyrus / cingular sulcus
9. L anterior amygdalia	27. L anterior cingulate gyrus
10. L hippocampus—head	28. L frontal superior gyrus
11. L hippocampus—anterior	29. L frontal superior gyrus
12. L hippocampus—body	30. L frontal superior gyrus
13. L white matter / hippocampus (posterior)	31. L front superior gyrus / arachnoide space
14. L white matter	32. L perimeningeal space
15. L white matter	
16. L temporo-occipital sulcus	
17. R medial gyrus	
18. R anterior cingulate gyrus	

* R = right hemisphere; L = left hemisphere.

limbic and fronto-cingulate trajectories. The positions of the electrodes obtained from IRM are given in Table I. The task was a classic visual oddball discrimination: a panel of 80 red-light diodes (targets) was lighted randomly interleaved with 320 green diodes (nontargets). The stimuli were turned on for 40 ms, with an interstimulus interval varying randomly between 800 ms and 1,200 ms. The patient had to press a button in response to target stimuli only. Electrical data were recorded relative to an average reference.

In a previous study of gamma emission from comparable human data using the same protocol, we had found that a specific response around 45 Hz is triggered specifically by the stimuli [Lachaux et al., 1999a]. Accordingly, we focused our study of PLS only around this frequency.

Results

The matrices of PLS values for all pairs of electrodes and both target and nontarget stimuli are shown in Figure 4 (see legend for conventions). As for the stimulation effect, significant synchronies are slightly more common between left hippocampus and frontal-cingulate regions. On the whole, however, the synchrony patterns are roughly comparable for both conditions, although slightly increased for the nontarget condition. It is important to make it clear that our purpose here was *not* to study in detail the neurosignificance of phase-locking related to the visual task performed by the subject. This would entail a careful analysis of the time courses of synchrony and of the differences between target vs. nontarget, following Rodriguez and colleagues [1999]. For subject PI, such a study is made difficult by the clinical constraints for electrode placement, preventing a choice of positions that would be more consonant given the chosen cognitive task. Thus we find only a very limited change in synchrony over time and between conditions. Accordingly, our aim here is more modest: to apply our method to real signals (subdural LFP potentials) in order to verify the existence of stimulus-triggered gamma synchronies between electrodes from signals of this intermediate level of resolution (as compared to scalp recordings) and to distinguish between short-range and long-range synchrony.

Local synchronies. If we first focus on the short range for synchronies found within the same region of electrodes (limbic or frontal, left or right), it is easily seen that the intensity of phase-locking (quantified by PLV) decreases steadily with interelectrode separation. For instance, in the right limbic recordings of this patient (which correspond to a necrotic hippocampus where the epileptic focus was diagnosed), synchrony extends up to interelectrode distances of up 8 cm (Fig. 5).

However, these observations are an artifact due to the fact that neighboring electrodes simply will record the *same* field potential due to volume conduction and are thus trivially synchronous. To distinguish between volume conduction and true synchrony is actually the main difficulty that limits the understanding of synchrony at short range. The right hippocampus contains damaged tissues with a higher conductivity than normal, thus enhancing volume conduction locally. In contrast, in the left limbic region, synchrony decreased much *faster* with electrode separation, and it did not extend beyond 2 cm. This result coincides very well with the findings by Menon et al. [1996] on normal human subdural recordings, showing that short range synchrony decreased sharply after 2 cm of interelectrode distance. They explained these results by strong local lateral connections that would induce synchronization of neighboring neurons within the 2 cm radius. In our view, simple passive volume conduction also may create such spurious synchrony (see next section).

Long-range synchronies. In contrast with synchrony *within* regions (short-range synchrony), synchrony *between* locations (long-range synchrony) varied in time

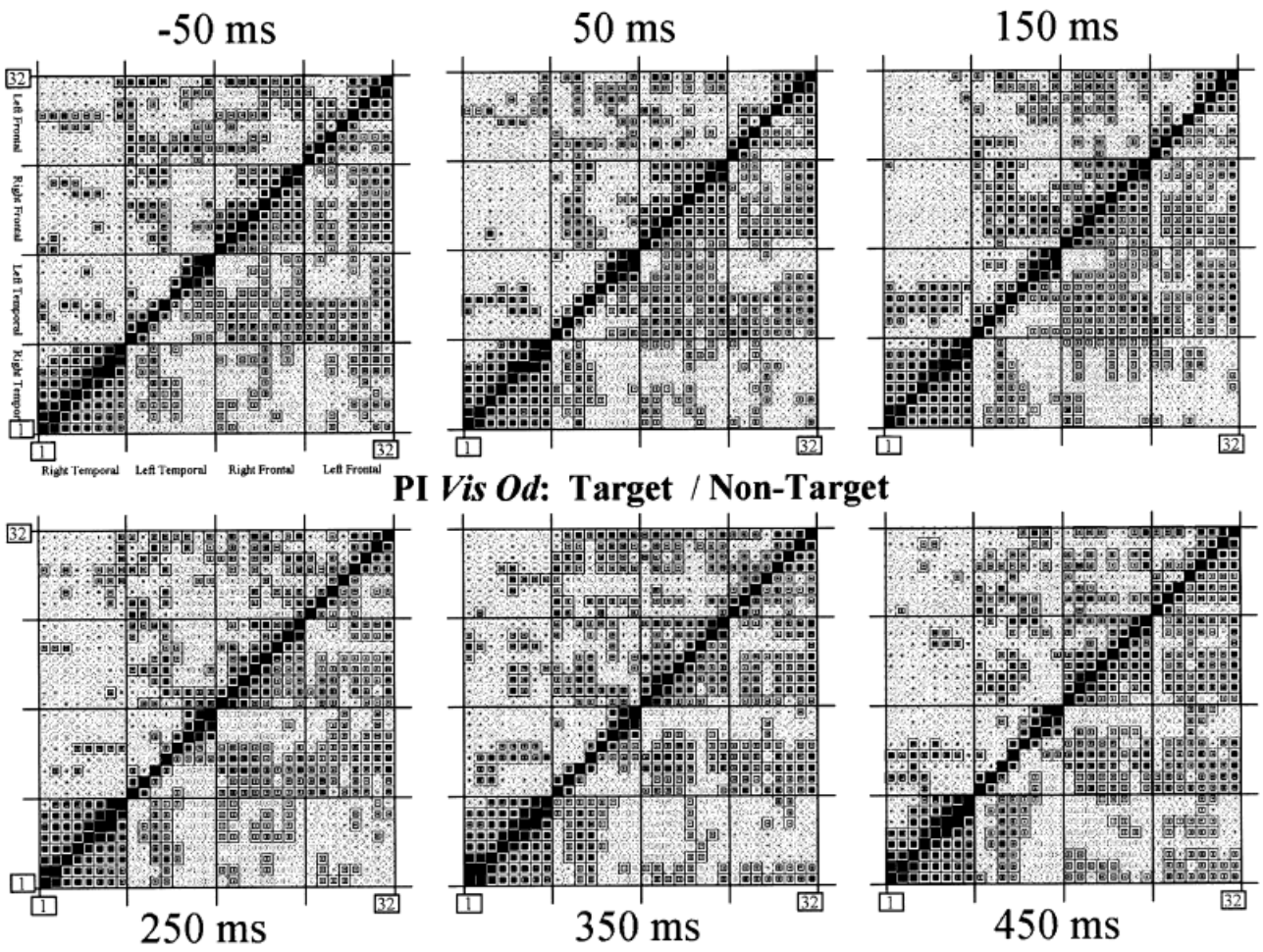

Figure 4.

PLV values for subject PI. Values are presented for six consecutive time windows (stimulation occurs at zero ms). Boxes above diagonal (up-left) correspond to the target stimulation; those under diagonal (down-right) to nontargets. Each box represents the synchrony value for an electrode pair. If synchrony does not reach significance, the box is filled by a circle with a dot in the center. When it reaches significance threshold (PLS $<$ 0.05), the square is filled to an extent proportional to the PLV value.

and occurred only between specific pairs of electrodes with no relation to interelectrode separation. For instance, the right-limbic vs. left-frontal quadrant of the matrix in Figure 4 shows the localized emergence and disappearance of synchronies over time. The timing of this pair is quite different from its converse, with the left-limbic region.

We conclude that these observations are convincing evidence that significant long-range synchronies are established during this cognitive task involving deep limbic and frontal regions. These synchronies cannot be explained by volume conduction; it seems more likely that they represent a partial correlate of the functional integration mechanism during visual discrimination. A detailed account and cognitive analysis of long-range synchronies in intracortical recordings of several epileptic patients will be presented elsewhere. The present results, along with previous reports [Bressler et al., 1993; Desmedt and Tomberg, 1994; Friston et al., 1997; Roelfsema et al., 1997], strongly support the view that gamma synchrony acts as distributed unifying mechanism [Rodriguez et al., 1999].

SEPARATING SYNCHRONY FROM VOLUME CONDUCTION

As noted above, synchrony between two macro recordings is not always due to neural interactions. Whereas animal studies of synchrony are based on the coincidence of *spikes* recorded from microelectrodes (single or multiunit recordings), human studies use surface or implanted electrodes that integrate neural

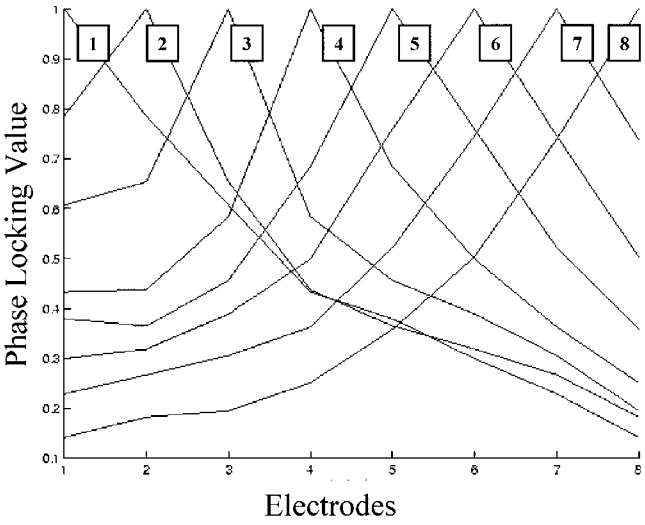

Figure 5.
PLV as a function of distance for the right temporal electrodes of subject PI. A regular 1 cm spacing separates eight electrodes. The synchrony decreases almost linearly from 1 to 0 when the interelectrodes distance increases.

activity over large volumes. When the volumes recorded by two electrodes overlap, the shared neuronal population creates spurious synchrony between the signals (see Appendix). Here, we discuss ways to reduce such synchrony due to volume conduction (or "conduction synchrony") better to identify synchrony due to actual neural couplings ("true synchrony"). Two factors are important to examine: (1) volume conduction, and (2) an inappropriate choice of the reference electrode.

Influence of volume conduction on synchrony

Separation between conduction synchrony and true synchrony. The separation between these two types of synchrony is difficult because they can occur at the same latencies and in the same frequency range (Fig. 4). This contradicts a common assumption that conduction synchrony should be broad-band and roughly constant in time, whereas true synchrony should be more specific. Another common assumption is that the phase difference between electrodes should be zero in case of conduction synchrony. This is usually false: even if two electrodes record the same group of sources, the signals of these electrodes are different linear combinations of the sources amplitudes, because each source is recorded by the two electrodes in two different ways that depend on the relative position of the source and the electrodes. Therefore, the phase of the signals recorded by the two electrodes should be different, except if all the sources have the same phase.

One can still suggest a rule of thumb based on intersite comparison. If volume conduction creates high synchrony between two electrodes, then high synchrony also should be observed between their neighbors. In other words, in general, *when there is synchrony due to diffusion, there should be diffusion of synchrony.* This diffusion of synchrony is precisely the effect shown in Figure 4 within regions, but not between them. Yet, this rule of thumb falls short of providing a reliable test to identify conduction synchronies.

Reducing volume conduction. Since there is no universal rule to distinguish true synchrony from conduction synchrony, one must rely on recordings with high spatial resolution in which the overlap between the brain volumes recorded by different probes is minimum. In this sense, subdural recordings constitute an ideal study case. To study normal subjects, the use of EEG or MEG is the most common option. MEG should be preferred: volume effects are less severe because the head tissues induce no diffusion of the magnetic field, in contrast with electrical potential [Hämäläinen et al., 1993]. Also, the amplitude of the magnetic field decreases faster with distance than the electrical potential, so that the volume recorded by an EEG electrode is larger than that recorded by a MEG sensor. In addition, the spatial resolution of MEG can be increased before estimating synchronies [Friston et al., 1997].

Still, most studies turn to EEG data since MEG remains a rare and expensive technique and because EEG can record sources configuration not recorded by MEG. Two main techniques have been used to improve the spatial precision of EEG: (1) inverse deblurring [Le and Gevins, 1993], and (2) the derivation of the scalp current density profiles (SCD) [Pernier et al., 1988]. We tested on a simulation the efficiency of both methods for the study of synchrony from surface EEG recordings.

This simulation mimics the experimental setting of a classic EEG sensory task in which 50 repetitions of the same stimulus generate independent responses in two cortical locations. We selected two independent series of 50 recordings from subject PI and used them as amplitudes of two sources placed in a spherical model of the head [for details see Lachaux et al., 1997]. This three-layered model comprised: (1) brain (conductivity = 1, arbitrary units; radius = 8.5 cm), (2) skull (conductivity = 0.0128; radius = 9.2 cm), (3) skin (conductivity = 1; radius, 10 cm) (infinite reference: potential is zero far from the sphere). Electrical sources were expressed as two dipoles with radial orientations with respect to the scalp, located in two superficial symmet-

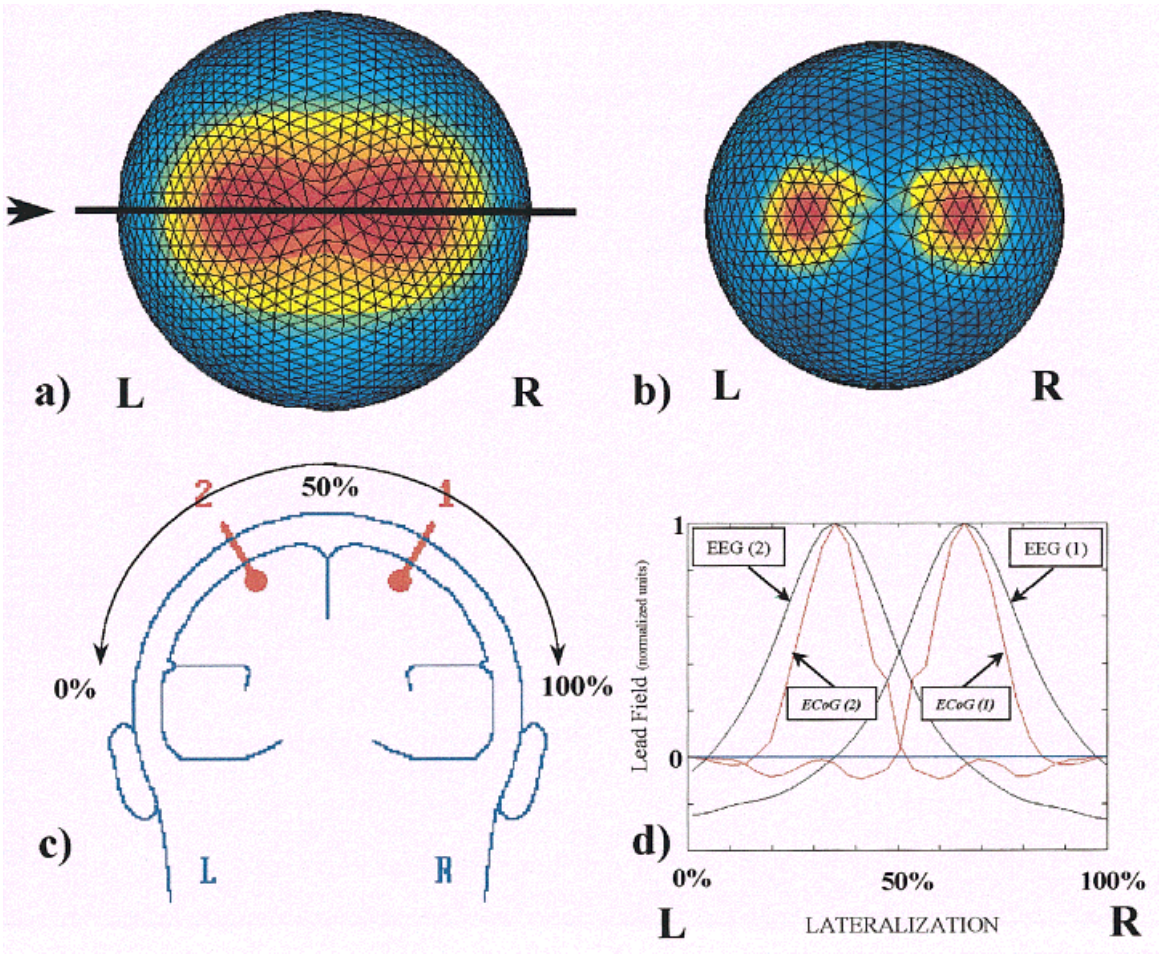

Figure 6.

Simulation of an EEG and its corresponding ECoG. Two radial dipoles were placed in symmetric positions in the (T7-Cz-T8) plane, containing both ears and the head's vertex (**c**). EEG generated by these dipoles was computed, and ECoG reconstructed using a deblurring technique. (**a**) EEG cartography for two dipoles with same amplitude (**b**) corresponding ECoG. (**d**) EEG and ECoG contributions of each dipole as a function of laterality along a T7-Cz-T8 axis.

ric positions in each hemisphere (see Fig. 6). The surface activity induced by these dipoles was computed (forward calculation) using the software BESA [Scherg, 1990] in 55 scalp positions for all 50 trials.

The EEG thus obtained was treated by a variation of the deblurring technique originally proposed by Le and Gevins [1993] to calculate the corresponding ECoG (backward calculation). Using BESA, we also computed the potential generated by the two dipoles on the cortex (i.e., the true EcoG, forward problem) to check the accuracy of the ECoG reconstructed by deblurring. The dipole model and the corresponding EEG and ECoG are shown in Figure 6.

We then computed the phase-locking values for the scalp and cortical positions lying on a left-right axis (T7-Cz-T8). For comparison, we computed the scalp current density on this spherical model [Pernier et al., 1988] and the PLV between the SCDs at these same scalp positions (Fig. 7, EEG and ECoG; Fig. 8, SCD). Since the sources of this model were independent, all significant PLS were due to conduction synchrony.

As shown in Figure 7, deblurring sharpened the borders of synchronous regions and reduced spurious synchronies (Fig. 7). SCD produced comparable effects, but slightly less detailed. Therefore, these methods seem useful first steps before the estimation of synchrony from EEG recordings. In practical cases, SCD may be preferred because its computation is much simpler than deblurring. Precise deblurring requires a description of the geometry and the conductivity of each individual's skull and skin.

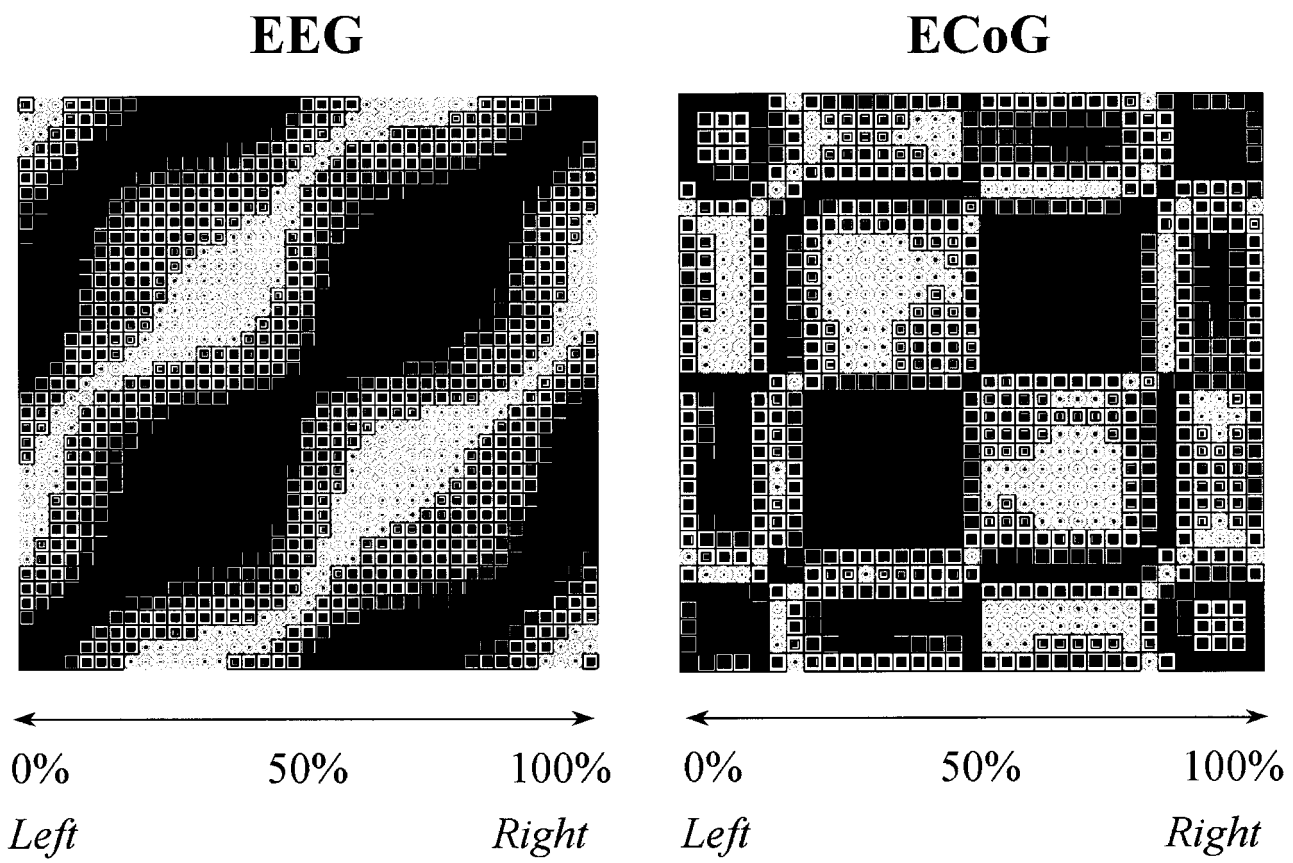

Figure 7.

PLV values for simulated EEG and ECoG. Using the same presentation as for Figure 5, PLV is presented for n electrodes lying on the T7-Cz-T8 lines. Electrodes are referred by their position along this axis from left (left ear) to right (right ear). For some electrode pairs, synchrony is significant between a and b (up-left part of the matrix), but not between b and a (bottom-right part of the matrix). In other words, maps are not rigorously symmetric. This is because the surrogate PLV distributions are not strictly the same in the two cases, and thus the 5% significance thresholds may be slightly different.

In a recent study, Nunez and colleagues [1997] tested the effect of volume conduction on the correlation between electrodes and found converging conclusions. Independent distributed sources were simulated in a volume conductor model of the head, the corresponding EEG was calculated in 64 scalp positions, and the squared correlation coefficient was computed as a function of interelectrode separation. Granted, correlation coefficient is not a close estimate of synchrony; Nunez et al. [1997] also suggested using SCD or EcoG estimations to reduce conduction interactions.

Influence of the reference-electrode on synchrony

Apart from volume conduction, the other major problem in synchrony estimation is the choice of the reference electrode. This problem uniquely concerns EEG; another reason to prefer the MEG technique. For electric recordings, a review of the literature on frequency coherence provides no general agreement on the optimal reference. In the present study, we took an average reference to study epileptic data and an infinite reference in the electrocorticogram simulation.

Figure 9 shows results obtained with other references. When subtracting a reference term, it is not clear whether synchrony should decrease (because a common part of the signals is removed), or increase (because a common term is artificially added to all the signals). When studying EEG, the computation of scalp current density is often a way to solve the reference problem, because spatial derivation makes this term disappear. But our simulations (Fig. 9) show that this processing can create artificial synchronies. However, we used here spline interpolations to estimate SCDs [Pernier et al., 1988]; other approaches are possible and they may yield a better estimation [Lagerlund et al., 1995]. Nunez and colleagues [1997] proposed a detailed

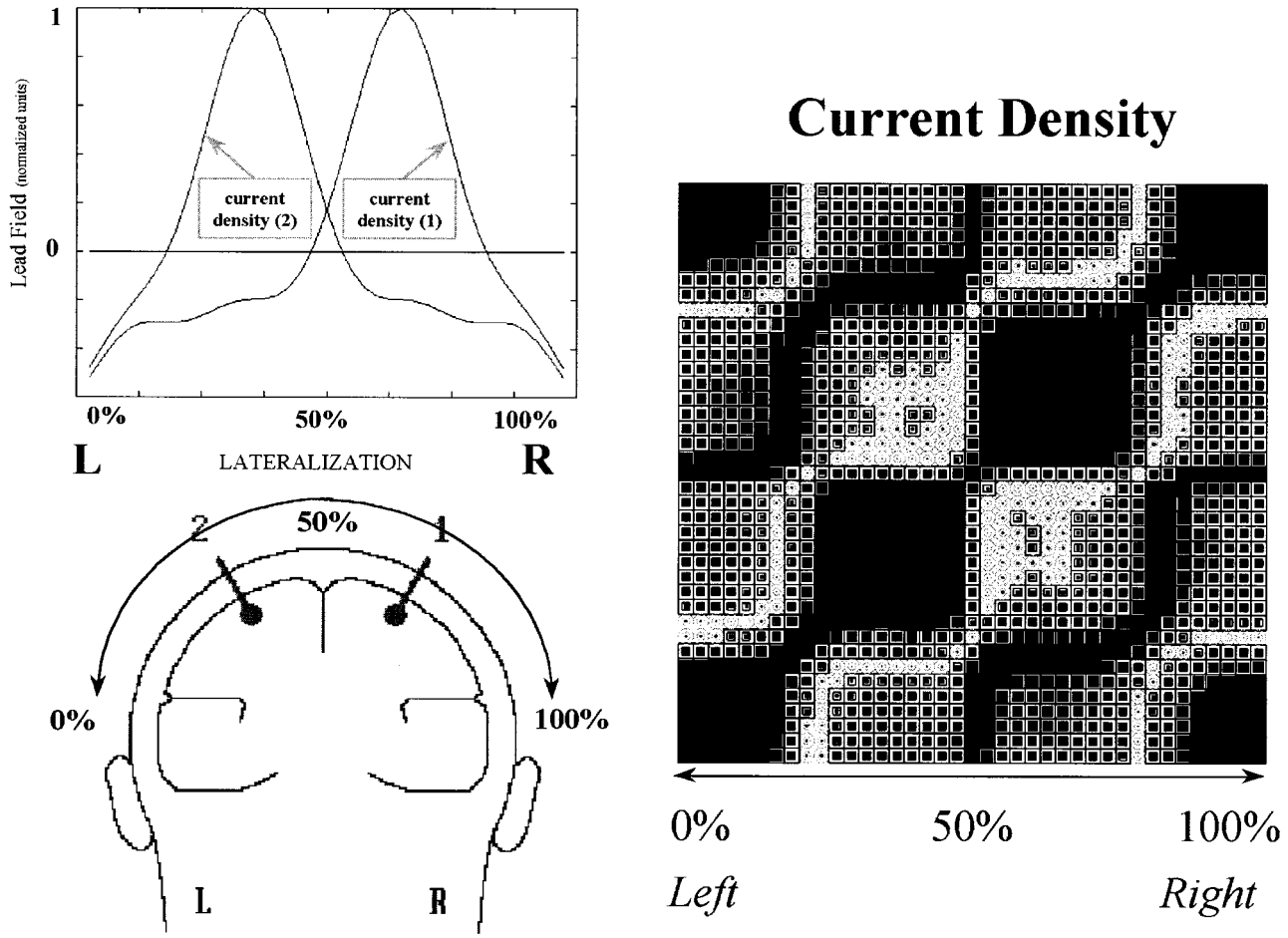

Figure 8.
PLV values for simulated scalp current density. SCD is computed from EEG presented on Figure 6. Up-left: Contributions of each dipole to SCD are presented as a function of laterality along a T7-Cz-T8 axis. Right: PLV values are presented for electrodes lying on this axis.

study of the influence of reference on interelectrode correlation coefficients. They argue that it is impossible to predict the effect of a reference on scalp coherence without both an accurate volume conductor model and a priori knowledge of all sources locations.

In brief, the question of the distinction between synchrony due to volume conduction and synchrony as functional neural integration is still inconclusive. Here, we note some steps in that direction, but none that provide a complete solution.

DISCUSSION

Narrow vs. broad frequency bands

One of the main limitations of the method presented here is that it depends crucially on the choice of a *specific* frequency for analysis in order to separate the amplitude and phase components of the signals. This separation is meaningless if one needs to work with a broad band. Further, choosing a given frequency needs filters with excellent resolutions in both time and frequency, which do not change the phase. (Our choice, a classic finite impulse response filter, may not be optimum.)

Yet, a careful time frequency analysis of intracortical and scalp data shows that their spectral content is very broad (between 0–80 Hz0, and the relative amplitudes varies considerably over time during an experimental situation [Tallon-Baudry et al., 1997; Lachaux et al., 1999a; Rodriguez et al., 1999]. It is of the greatest interest to investigate if there are interactions between frequencies located in different bands and what, if any, is their functional significance. PLS permits only a

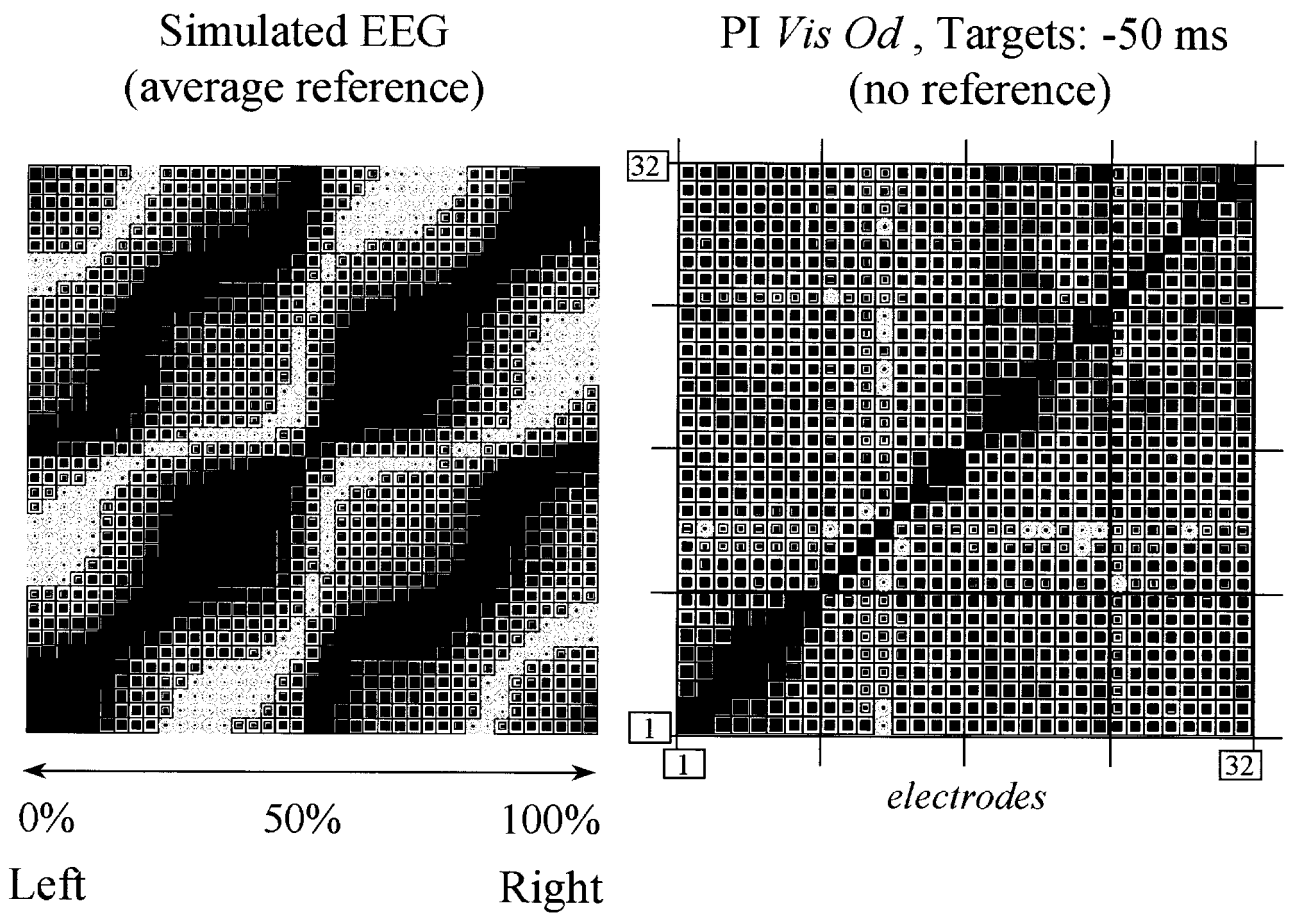

Figure 9.
Effect of reference electrode on PLV values. We computed PLV for the simulated EEG data presented in Figure 7, using an average electrode (left), instead of the infinite reference used for Figure 7. We also computed synchrony for subject PI for both stimulation conditions using no reference instead of average reference; spurious synchronies appear for almost all pairs.

limited answer to these questions, since the same analysis can be repeated over several bands. However, a complete answer would require a method based on a broad-band calculation of synchrony. Such an approach takes us far away from classical methods, but is an active area of study in mathematical physics.

Average vs. single trial

A second important limitation of the method introduced here is that it focuses on the detection of phase-locking between pairs recordings *across trials:* i.e., the likelihood that phase-difference between the oscillations of two neural populations remains the same *from trial to trial* for a given delay in time. This excludes those synchronies that are not established with a fixed delay from trial to trial. In order to extract such information, one needs to introduce averaging or smoothing procedures over time and to work on the basis of *single* trials, not averages. An analogy for the study of gamma band emission can be helpful here. PLS can be compared to the procedures that detect the evoked gamma emission, but fail to detect the induced responses. In fact, induced responses are not stimulus locked and thus require a trial by trials analysis to construct a probability distribution [Tallon-Baudry et al., 1997; Lachaux et al., 1999a]. PLS cannot detect this second type of single-trial phase locking if the phase-difference varies in latency between trials.

The detection of this second type of phase-locking in single trials is possible using a recent technique, *smoothed phase locking statistics* (SPLS) that we have introduced recently [Lachaux et al., 1999b]. The application of this improved approach will tell, in time, if

functional neural synchronies are more common than we have shown in this report.

NOTE ADDED IN PROOF

After this paper was sent for publication, a recent publication introduced an alternative method to compute phase synchorny between bivariate data based on the Hilbert transform (Tass et al., *Physical Rev Letters* **81**:3291–94, 1998). The two approaches are comparable in several respects. A study of their comparative advantages is being carried out.

ACKNOWLEDGMENTS

This work began a few years ago thanks to the essential contribution of Johannes Müller-Gerkin on MSC calculations. Our thanks also to Laurent Hugueville for his help on EcoG methods.

REFERENCES

Bressler SL, Coppola R, Nakamura R. 1993. Episodic multiregional cortical coherence at multiple frequencies during visual task performance. Nature 366:153–156.

Bullock TH, McClune MC. 1989. Lateral coherence of the electrocorticogram: A new measure of brain synchrony. EEG Clin Neurophys 73:479–498.

Clifford Carter G. 1987. Coherence and time delay estimation. Proceedings of the IEEE 75:236–255.

Damasio AR. 1990. Synchronous activation in multiple cortical regions: A mechanism for recall. Seminars in Neurosci 2:287–296.

Desmedt JE, Tomberg C. 1994. Transient phase-locking of 40 Hz electrical oscillations in prefrontal parietal cortex reflects the process of conscious somatic perception. Neurosci Lett 168:126–129.

Fisher NI. 1993. Statistical Analysis of Circular Data. Cambridge: Cambridge University Press.

Friston KJ, Stephan KM, Frackowiak RSJ. 1997. Transient phase-locking and dynamic correlations: are they the same thing? Hum Brain Mapp 5:48–57.

Gray CM, Konig P, Engel AK, Singer W. 1989. Oscillatory responses in cat visual cortex exhibit inter-columnar synchronization which reflects global stimulus properties. Nature 338:334.

Grossman A, Kronland-Martinet R, Morlet J. 1989. Reading and understanding continuous wavelets transforms. In: Combes JM, Groosmsman A, Tchamitchian P (eds): Wavelets, Time-frequency Methods and Phase Space. Berlin: Springer-Verlag, pp 2–20.

Hämäläinen M, Hari R, Ilmoniemi RJ, Knuutila J, Lounasmaa OV. 1993. Magnetoencephalography: Theory, instrumentation, and applications to noninvasive studies of the working human brain. Rev Mod Phys 65:

König P, Engel AK, Singer W. 1995. Relation between oscillatory activity and long-range synchronization in cat visual cortex. Proc Natl Acad Sci USA 92:290–294.

Lachaux J-Ph, Pezard L, Garnero L, Pelte C, Renault B, Varela FJ, Martinerie J. 1997. Spatial extension of brain activity fools the single-channel reconstruction of EEG dynamics. Hum Brain Mapp 5:26–47.

Lachaux JP, Rodriguez E, Martinerie J, Adam C, Hasboun D, Varela FJ. 1998. Gamma-band activity in human intracortical recordings triggered by cognitive tasks. Submitted to Europ. J. Neurosci.

Lachaux J-P, Hurtado JM, Sigvart K, Varla FJ, Gray CM. 1999b. Measuring coherence between brain signals: A new method for single-trial analysis. J Comput Neuroscience (submitted)

Lagerlund TD, Sharbrough FW, Busacker NE, Cicora KM. 1995. Interelectrode coherences from nearest-neighbor and spherical harmonic expansion computation of laplacian of scalp potential. Electroencephalogr Clin Neurophysiol 95:178–188.

Le J, Gevins A. 1993. Methods to reduce blur distorsion from EEG's using a realistic head model. IEEE Transact BioMed Eng 40:517–528.

Le Van Quyen M, Adam C, Lachaux JP, Martinerie J, Baulac M, Renault B, Varela FJ. 1997. Temporal patterns in human epileptic activity are modulated by perceptual discriminations. Neuroreport 8:1703–1710.

Menon V, Freeman WJ, Cutillo BA, Desmond JE, Ward MF, Bressler SL, Laxer KD, Barbaro N, Gevins AS. 1996. Spatio-temporal correlations in human gamma band electrocorticograms. Electroencephalogr Clin Neurophysiol 98:89–102.

Müller-Gerking J, Neuenschwander S, Martinerie J, Pezard L, Renault B, Varela FJ. 1996. Detecting non-linearities in neuroelectrical signals: A study of synchronous local field potentials. Physica D 94:65–91.

Neuenschwander S, Engel A, König P, Singer W, Varela F. 1996. Synchronization of neuronal responses in the optic tectum of awake pigeons. Visual Neurosci 13:575–584.

Nunez PL, Srinivasan R, Wetdorp AF, Wijesinghe RS, Tucker DM, Silberstein RB, Cadusch PJ. 1997. EEG coherency I: Statistics, reference electrode, volume conduction, Laplacians, cortical imaging and interpretation at multiple scales. EEG Clin Neurophys 103:499–515.

Pernier J, Perrin F, Bertrand O. 1988. Scalp current densities: Concept and properties. Electroenceph Clin Neurophysiol 69:385–389.

Rodriguez E, George N, Lachaux JP, Martinerie J, Renault B, Varela F. 1999. Perception's shadow: Long-distance synchronization of human brain activity. Nature 397:430–433.

Roelfsema PR, Engel AK, König P, Singer W. 1997. Visuomotor integration is associated with zero time-lag synchronization among cortical areas. Nature 385:157–161.

Scherg M. 1990. Fundamentals of dipole source potential analysis. In: Grandori F, Hoke M, Roamni GL (eds): Auditory Evoked Magnetic Fields and Potentials: Advances in Audiology, Vol 6. Basel: Karger, pp 40–69.

Singer W, Gray CM. 1995. Visual feature integration and the temporal correlation hypothesis. Annu Rev Neurosci 18:555–586.

Tallon-Baudry C, Bertrand O, Delpuech C, Pernier J. 1996. Stimulus specificity of phase-loked and non-phase-locked 40 Hz visual responses in human. J Neurosci 16:4240–4249.

Tallon-Baudry C, Bertrand O, Delpuech C, Pernier J. 1997. Oscillatory gamma-band (30–70 Hz) activity induced by a visual search task in human. J Neurosci 17:722–734.

Theiler J, Eubank S, Longtin A, Galdrikian B, Farmer D. 1992. Testing for nonlinearity in time series: The method of surrogate data. Physica D 58.

Tononi G, Edelman M. 1998. Consciousness and complexity. Science 282:1846–1851.

Varela FJ. 1995. Resonant cell assemblies: A new approach to cognitive functions and neuronal synchrony. Biol Res 28:81–95.

APPENDIX

Source of spurious synchronies

Here, we consider how volume conduction can induce spurious correlations between electrode potentials. For this purpose, we consider a set of microelectrodes located within a brain area to record local-field potentials produced by an assembly of neurons with *uncorrelated* activities.

In response to a stimulation s, each neuron has an activation $p(x, t, s)$, which is a function of its position x, time t, and s. Suppose to fix ideas that $p(x, t, s)$ is a white-noise such that the mean value of $p(x, t, s)^2$ over time is unity. Since the neurons have uncorrelated activities, the mean value of $p(x, t, s) \cdot p(x', t, s)$ across time and trials (we note it $\langle p(x) \cdot p(x') \rangle$) is then δ(x, x1), (i.e., 1 if $x = x'$, 0 if not).

The local-field potential recorded by an electrode located in y, can be expressed as a linear combination of the sources amplitudes:

$$e(y, t, s) = \int h(y, x) \cdot p(x, t, s) dx.$$

We consider further that all the electrodes are roughly located at the same distance around the sources, so that $\langle e(y) \rangle$ is roughly the same for all the electrodes. Thus we get a fair approximation of the correlation between the potentials in two positions y and y′ by computing $\langle e(y) \cdot e(y') \rangle$. This is done as follows. For any time t and sample s,

$$e(y, t, s) \cdot e(y', t, s) = \left(\int h(y, x) \cdot p(x, t, s) \cdot dx \right) \cdot \left(\int h(y', x') \cdot p(x', t, s) \cdot dx' \right)$$

or

$$e(y, t, s) \cdot e(y', t, s) = \int \int h(y, x)\, h(y', x') \cdot p(x, t, s) \cdot p(x', t, s)\, dx dx'$$

so that when averaging,

$$\langle e(y) \cdot e(y') \rangle = \int \int h(y, x)\, h(y', x') \cdot \langle p(x) \cdot p(x') \rangle\, dx dx'$$

or,

$$\langle e(y) \cdot e(y') \rangle = \int \int h(y, x)\, h(y', x') \cdot \delta(x, x')\, dx dx'$$

finally,

$$\langle e(y) \cdot e(y') \rangle = \int h(y, x)\, h(y', x)\, dx.$$

Thus due to volume-conduction, $\langle e(y) \cdot e(y') \rangle$ is non-zero even if there is no correlation at all between the two sources of activities.